

PROCEEDINGS OF SPIE

[SPIDigitalLibrary.org/conference-proceedings-of-spie](https://spiedigitallibrary.org/conference-proceedings-of-spie)

High numerical aperture multimode fibers for prime focus use

Kaiyuan Zhang, Jessica R. Zheng, Will Saunders

Kaiyuan Zhang, Jessica R. Zheng, Will Saunders, "High numerical aperture multimode fibers for prime focus use," Proc. SPIE 9912, Advances in Optical and Mechanical Technologies for Telescopes and Instrumentation II, 99125J (22 July 2016); doi: 10.1117/12.2232131

SPIE.

Event: SPIE Astronomical Telescopes + Instrumentation, 2016, Edinburgh, United Kingdom

High Numerical Aperture Multimode Fibers for Prime Focus Use

Kaiyuan Zhang^{1, 2}, Jessica R. Zheng¹, Will Saunders¹

¹) Australian Astronomical Observatory, 105 Delhi Road, North Ryde, NSW 2112, Australia

²) Nanjing Institute of Astronomical Optics & Technology, National Observatories,
Chinese Academy of Science, 188 Bancang Street, Nanjing 210042

ABSTRACT

Modern telescopes typically have prime focus speeds too fast for direct use with standard numerical aperture (NA=0.22±0.02) silica-cored fibers. Specifically, the current design for the proposed Maunakea Spectroscopic Explorer (MSE) telescope is $\sim f/1.93$, requiring fibers with NA>0.26. Micro fore-optics can be used to slow the beam, as used on the prime focus spectrograph (PFS) on Subaru, but this adds cost and complexity, and increases losses. An attractive alternative is offered by high NA pure silica-cored fibers, which can be used directly, and which are now available from multiple vendors. We present throughput and focal ratio degradation measurements on two samples of these high NA fibers. It is found that the measured attenuation losses are comparable with the best available standard NA fibers. The fibers were also tested for focal ratio degradation, and the fiber from CeramOptec was found to have acceptable FRD, representing additional collimator losses $\sim 1\%$. The near field performance of the high NA fiber is also investigated and these high NA fibers exhibit very good scrambling performance; no evidence for significant output near-field variations was observed for plausible input beam position or angle variations in a 50m fiber.

Keyword: FRD, optical fibers, high NA fiber, fiber spectroscopy, MSE

1. INTRODUCTION

Fibers are almost universally used in wide-field astronomical spectroscopy, because they allow the efficient use of remote bench-mounted spectrographs, allowing high spectral resolution and very large multiplex capabilities, at reasonable cost. Like other massively multiplexed spectroscopic telescopes (4MOST, DESI, PFS), the Maunakea Spectroscopic Explorer (MSE) telescope depends on optical fibers to transfer the light from thousands of individual targets at the telescope focus to the spectrographs. For MSE, the same fibers must work over 370-1300nm, and preferably over 360-1800nm. Like PFS, the telescope focus is too fast to use standard NA=0.22 fibers directly. PFS will use micro-lenses at fiber input, but as well as adding complexity and cost, this causes geometric Focal Ratio Degradation (FRD), especially for fiber actuators with small ferrules, which allow very close target proximity – an important science goal for MSE.

Broadband multimode fibers with a NA high enough to accept the telescope beam directly are made by both Polymicro and CeramOptec. If either of these fiber types had suitable other characteristics for astronomical use – attenuation, near-field scrambling, and FRD performance – then this would be a very tempting route to take. Preliminary results from Pazder et al 2014[1] show promise, but also unexplained increase of FRD at large input angles.

In this paper, the performance of high NA fibers from both CeramOptec and Polymicro is investigated. The FRD is measured directly, by illuminating the fiber at different off-axis angles with a collimated incoherent beam, and measuring the full width half maximum (FWHM) of the resulting far-field annulus at output [2, 3]. This gives results more easily comparable between different experiments and fibers, than the equivalent measurement of the radius of encircled energy with filled input beam [4, 5, 6].

FRD has multiple causes: light scattering in the fiber, the core-cladding interface, micro and macro-bending of fiber; stress birefringence, and the imperfect quality of the fiber end face. A very large portion of the FRD is caused at the termination [5, 7]. Important factors here are whether the fiber has had the buffer stripped or not; the gap and concentricity between the fiber and ferrule, the type and amount of glue used, the ferrule length, and the fiber polish or cleave quality. In this paper, we investigated the FRD performance with those factors. For comparison, standard NA=0.22 fibers with identical length and diameter from both vendors are also investigated in the same fashion.

Even ignoring aperture and fiber tilt losses, fibers lose throughput in multiple ways. As well as collimator losses caused by FRD, there are Fresnel and scattering losses at input and output end surfaces, attenuation losses within the fiber caused by impurities and Rayleigh scattering, and evanescent losses from the cladding. For the latter, the usual rule-of-thumb is that the cladding should be thicker than 10λ [8], but as the NA of the input beam approaches that of the fiber, the required cladding thickness becomes infinite. The throughput is measured both as a function of incidence angle, and via a robust integrated measurement closely approximating real observations.

For precision spectroscopy, both near and far-field light distributions must be fully understood [3]. We investigate the variation of the centroid of the near-field light distribution at the output of fiber, when the incident beam is varied in angle and position.

2. THE TESTED FIBERS

200m-250m lengths of fiber with 100 μ m core diameter were obtained from both Polymicro and CeramOptec, in both high and standard NA types, with matching core/cladding/buffer diameters. The cladding thickness was 20 μ m for the CeramOptec fiber, but only 10 μ m for the Polymicro fiber, because a suitable preform was available. This was sufficient for our initial tests with optical light, even though it would not fulfil the usual 10λ rule out to 1.8 μ m. All fibers had polyimide buffer. The four fiber types tested are shown in Table 1. In each case, fibers were cut into long (50m) and short (2m) lengths, to try and isolate length-dependent effects from end effects.

Table 1. Fiber types tested

	Manufacturer	Core/cladding/buffer diameter	Nominal NA
P29	Polymicro	100/120/140	0.29
P22	Polymicro	100/120/140	0.22
C28	CeramOptec	100/140/170	0.28
C22	CeramOptec	100/140/170	0.22

To minimize stress and resulting FRD, we wanted to (a) avoid stripping the polyimide buffers if possible, (b) use close-fitting ferrules and (c) minimized glue usage. We purchased very well-matched customized ceramic ferrules, 144 μ m and 176 μ m ID for the 140 μ m and 170 μ m OD fibers, from Kientec systems, Inc. Glues used were Epoxy Tech 100-126-1 and ÅngströmBond® 9190. The latter gave slightly better results and all results quoted in this paper used it. After gluing, the fibers were machine polished with 30, 12, 9, 3, 1 and 0.3 μ m grit papers, identically for all fibers.

3. FRD MEASUREMENT

3.1. FRD test setup

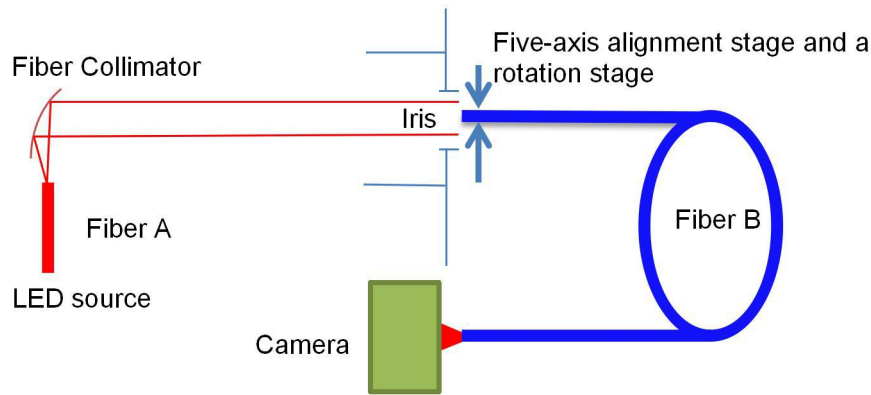


Figure 1: FRD measurement setup

The principle of the FRD test is to introduce incoherent collimated light into the fiber at a variety of input angles, and to measure the angular FWHM of the resulting far-field annulus of light output of the fiber. The experimental setup is shown in Figure 1. A LED is used as the light source, with wavelength 395nm, 505nm or 630nm. First the light is coupled into a multi-mode fiber A with core of 50 μ m and NA of 0.22. It is then collimated into a beam of diameter \sim 10mm by an off-axis mirror. The collimated light then illuminates the fiber B to be measured. The input end of fiber B is mounted on a rotation stage on top of a five-axis adjusting stage, by which the angle between the end of fiber B and the optical axis of the incidence collimated light can be adjusted. The far-field fiber output is measured with a FLI Microline camera with a 6644x4452 array of 5.5 μ m pixels. Figure 2 shows an example of the far field output image. The diameter of the circle represents twice the

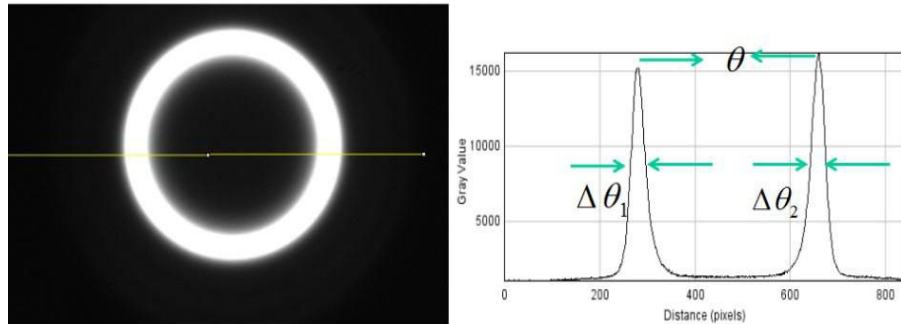


Figure 2: Far field output image

incidence angle and the full width of half maximum (FWHM) of the ring represents the measured FRD. The centroid of the far field distribution is first estimated and the ring summed in both horizontal and vertical axis across the estimated centroid as shown in Figure 2.

We split the cross section into 4 parts by its two peaks and one middle valley. The angular FWHM of the FRD ring is calculated as:

$$FRD = w \frac{\Delta\theta_1 + \Delta\theta_2}{\theta} \quad (1)$$

where θ is the diameter of the circle and $\Delta\theta_1$ and $\Delta\theta_2$ are the FWHM of the left and right parts of the ring, all measured in pixels, and w is the input angle in degrees. To determine the normal incidence angle of the input beam before testing the FRD at different incidence angle, firstly we align the 5-axis stages to optimize the fiber

output power and align the center of the front end of fiber to the vertex of the rotation stage. By adjusting the rotation stage, the incidence angle of input beam can be turned from negative to positive angle, the output power from the fiber is monitored as shown in Figure 3, and the maximum output power which is corresponding to the normal incidence angle is obtained.

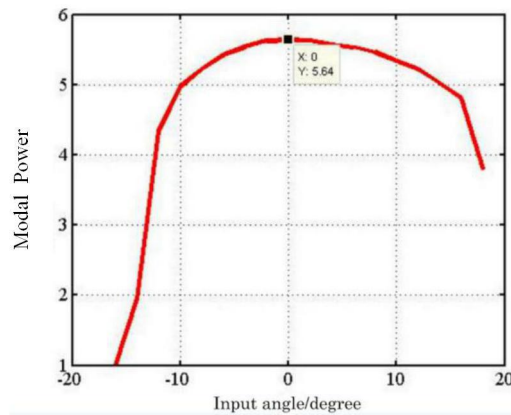


Figure 3: Fiber output power at different incidence angle

3.2. Measured FRD

Figure 4 shows the measured FRD ring image of 50m lengths of high NA fiber from both Polymicro and CeramOptec, with the same incidence angle of 16° ; the cross section profiles are also shown. Clearly, the FRD ring from the CeramOptec high NA fiber is much sharper than the Polymicro fiber, reflecting better FRD performance.

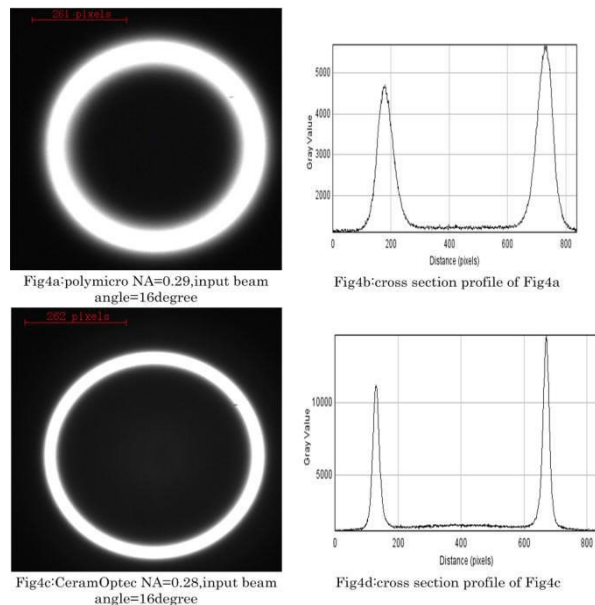


Figure 4: Far field image with collimated beam input at 16° angle

Figure 5 shows the measured FRD vs different incidence angle from 10° to 16° , for both high NA and normal fibers, from both vendors. Both high NA and standard CeramOptec fiber has better FRD performance, and, for this batch at least, the Polymicro high NA fiber has rather poor FRD performance.

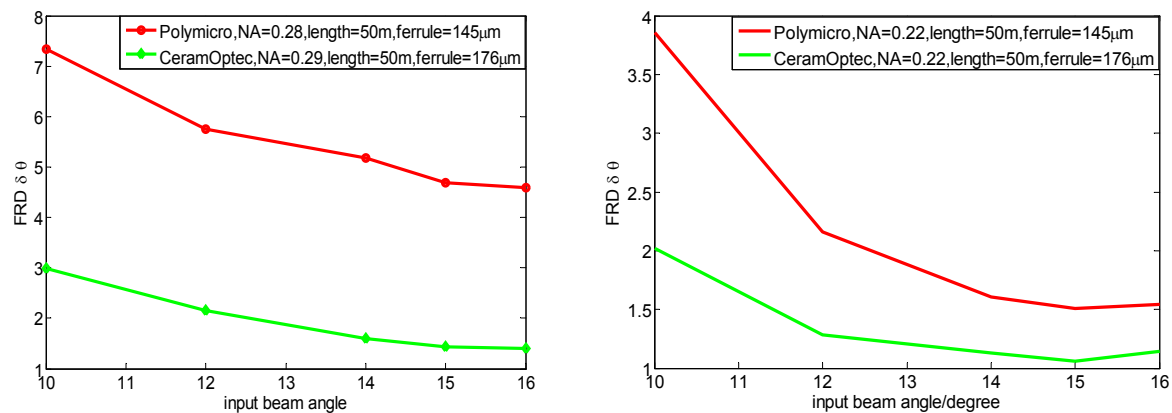


Figure 5: FWHM of the FRD annulus vs input angle, for 50m lengths of (a) high NA and (b) standard NA fibers. Note that the upturn at large angle in 5(b) is caused by exceeding the NA of the fiber.

The FRD results for the CeramOptec high NA fiber are not quite as good as for their standard NA fiber. However, in fractional terms (i.e. as a fraction of the maximum input angle), the results remain very good. Because the MSE primary is hexagonal, the input beam into the fibers is significantly apodized, even without FRD. This makes the system more tolerant to FRD than a circular primary. Figure 6 shows the modelled far-field output light distribution for a fiber on the telescope axis, without any FRD, and with the amount shown in Figure 6(b). The resulting light loss is <1% for plausible collimator speeds.

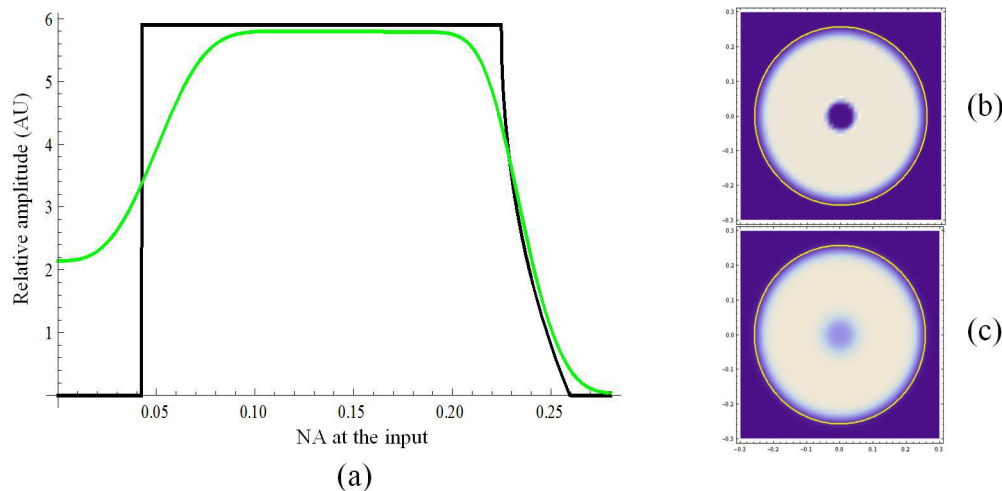


Figure 6: (a). Modelled radial profile of the MSE beam, without any FRD (black) and with the amount of FRD seen for the CeramOptec high NA 50m fiber (green). Figure 6(b), (c) a graphic representation of the same data. Yellow circle is nominal telescope speed (F/1.97).

4. MODAL THROUGHPUT MEASUREMENT

The FRD measurements described in the previous section also allowed a simple measurement of how throughput depends on input angle, just by summing the light in the FRD annuli. In particular, it should show how evanescent losses start to mount as the fiber NA is approached. The measurement cannot be very precise, because it is difficult to fix the axis of fiber rotation to be exactly at the tip of the fiber. Also, some decline with angle is expected, just because of the $\cos(\theta)$ projection effect at the input. Fresnel losses should not depend significantly on input angle at these angles. Figure 7 shows the throughput, normalized to that for an on-axis

collimated beam, for both high-NA fibers. The throughput shows a stronger decline with angle than expected, but little sign of the effect of the NA of the fiber. The overall throughput (reported in the next section is excellent), and this effect is reported mainly in the hope that a reader will offer an explanation.

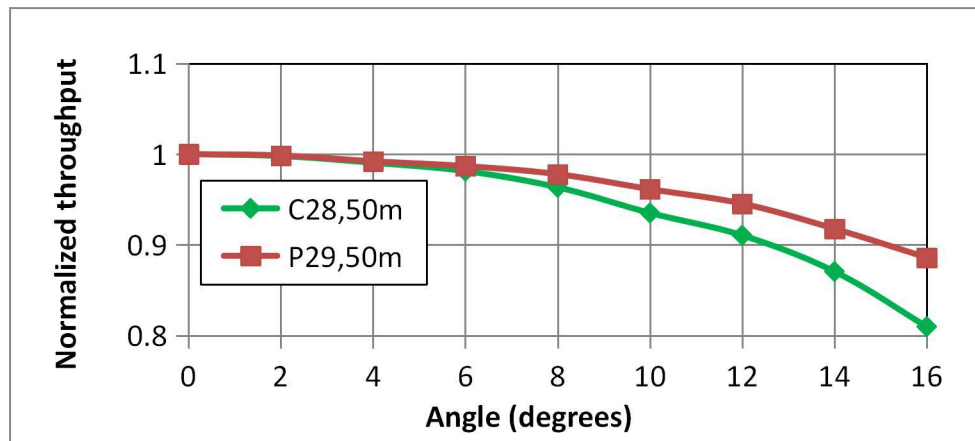


Figure 7: The light output from the fibers, when overfilled on input with a collimated beam at various angles. Normalization is to the on-axis value. All values have been divided by $\cos(\theta)$ to correct for the projection effect.

5. INTEGRATED THROUGHPUT MEASUREMENT

The throughput (as a function of input angle, wavelength, length) is a crucial parameter characterizing fiber performance. In the previous section, we tested and showed the normalized modal power transmission efficiency by using the collimated beam with different incidence angle. For telescope operation, the beam coupled into the fiber is a converging beam with a range of incidence angles. After some experimentation, we settled on a ‘MSE simulator’ consisting of a NA=0.25 spot focused on the end of the fiber, of size (FWHM=67 μm) somewhat smaller than the fiber diameter. The intention was to crudely mimic a stellar image on the fiber face. Figure 8(a) shows the experimental setup for the throughput measurement. The approximate fiber diameter is also shown as the circle at Figure 8(b).

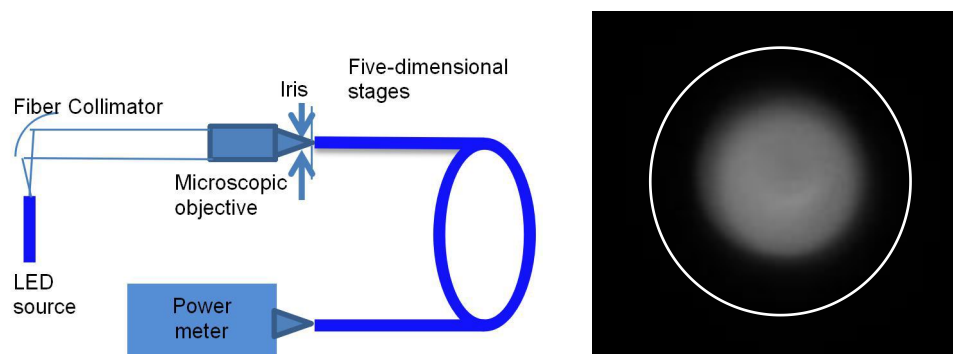


Figure 8: (a).Throughput measurement set up. (b). Resulting image on the output end face of fiber

The light from the light source of wavelength of 395nm, 505nm, 630nm, 1310nm and 1550nm was transmitted and collimated by a fiber collimator. The collimated light was focused by the objective lens with NA 0.25. The focused spot had $\sim 67\mu\text{m}$ diameter, as measured using our CCD camera with 10X microscopic lens.

To measure the throughput, the spot was first focused through a pinhole with diameter $100\mu\text{m}$, and the power measured after the pinhole with a power-meter. Then the pinhole was removed, and the focused beam coupled

into the 100 μ m core-diameter fiber, and power at the output end of fiber was measured. The ratio of these measurements gives us the throughput of the fiber. To disentangle the effects of attenuation and end-losses, the tests were repeated for 50m and 2m lengths of all fibers.

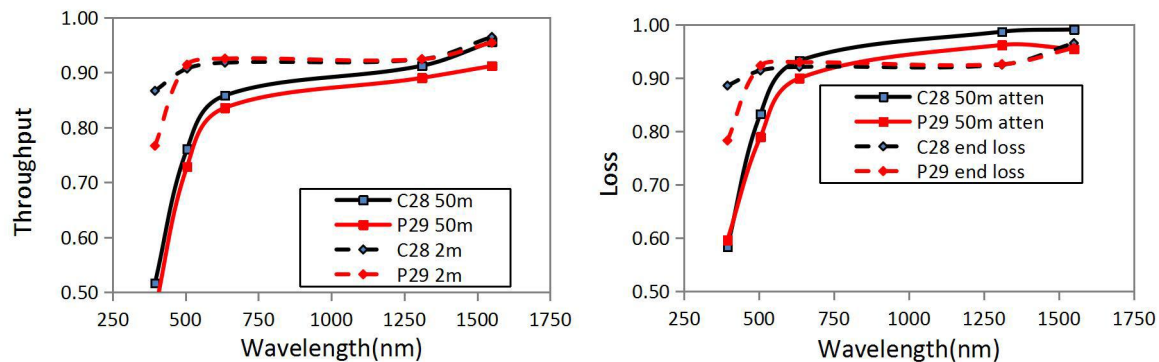


Figure 9: (a).Measured throughput for high NA fiber as a function of length, wavelength and manufacturer.
(b).Derived end and attenuation losses

Figure 9(a) shows the measured throughput results. The overall throughput for 50m fibers, including end-losses, varies from ~50% at 395nm to ~90% at 1550nm. The CeramOptec fiber is slightly better than the Polymicro. We can combine these results with those from the 2m fibers to separately estimate the end-losses and the attenuation. These are shown in Figure 9(b). This shows very consistent end-losses between manufacturers, but consistently better attenuation in the CeramOptec fiber. However, the measurement errors of a few 3% translate into large uncertainties in the NIR values. The attenuation losses are translated into dB/km in Figure 10, along with the nominal values supplied by the manufacturers. Uncertainties are a few dB/km. In the optical, our results are just slightly worse than the nominal values. In the NIR, our results are significantly better. The difference between manufacturers is small, but appears rather consistent with wavelength.

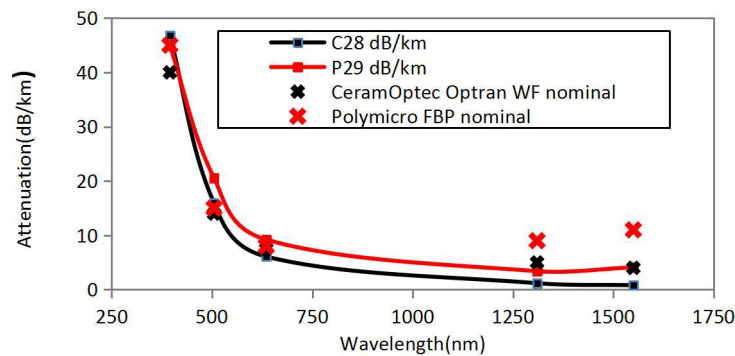


Figure 10: Derived attenuation for high NA fiber.

A concern with this measurement is that the underfilled input beam means that there are fewer skew modes than for a filled fiber, and in principle could misrepresent the throughput for a filled fiber. To test for this, we carried out the same experiment at 395nm for a fiber overfilled with an NA=0.25 beam. The results were almost identical.

We also measured the effect on throughput of tilting the NA=0.25 input beam. The results are shown in Figure 11. We found no measurable decline in throughput (<0.5%) for input angles \pm few degrees.

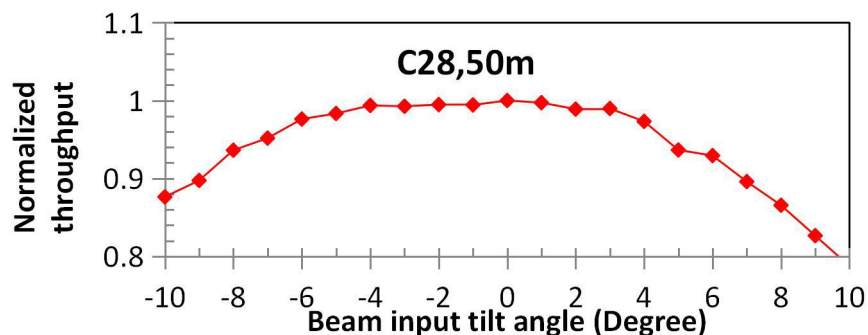


Figure 11. Normalized throughput for 50m CeramOptec fiber, with overfilled NA=0.25 input beam, as a function of input non-telecentricity.

The LEDs are not perfectly monochromatic. Figure 11 shows the nominal spectra of the 395nm LED. It is obvious that the typical peak is bluer than nominal, only specified to $\pm 6\text{nm}$; and there is significant light down to 380nm. Given the steep dependence of attenuation on wavelength in this regime, the true effective wavelength for the attenuation measurement is uncertain to within a few nm, but is likely to be blue-ward of 395nm, improving the actual attenuation. For the 1550nm measurement, the light source is laser rather than LED light.

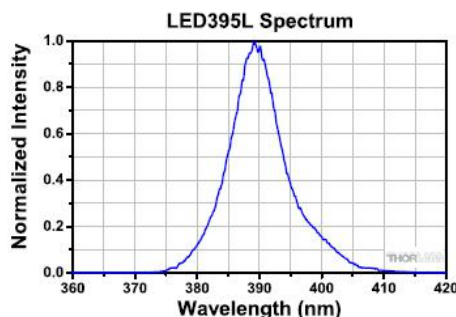


Figure 12: The spectra of the LED 395nm light source

6. NEAR FIELD PERFORMANCE MEASUREMENT

For astronomical use, consistency of the near field distribution at the fiber output is very important, as any change causes errors in the sky subtraction, and in the inferred spectral profile and velocity of the target. A desirable property of fibers is that the azimuthal distribution of light should be completely scrambled, in both near- and far-field for long length fibers [3]. To test for this effect, we constructed an experimental setup as shown in Figure 12. The fiber is mounted in the same way as in FRD measurement setup. The point source microscope (PSM) is used as the input beam source with a 10X microscopic lens of NA 0.25 to inject into the fiber, and the input fiber to the PSM is single mode fiber with core of $5.3\mu\text{m}$. Since the PSM is built with an input surface inspection tool, it is much easier for monitoring the relative input beam position on the fiber as shown in Figure 13. The other end of the fiber surface is re-imaged by an objective lens of NA 0.3 on a second CCD camera, and by calculating the image centroid; the near field performance can be verified.

Figure 14 shows the measured centroid of near field of high NA fiber of 2m long. We move the input beam from the edge of the fiber from one end to the other and do it in both horizontal and vertical axis by monitoring the input beam image on the PSM. The centroid measurement is measured with step of $10\mu\text{m}$.

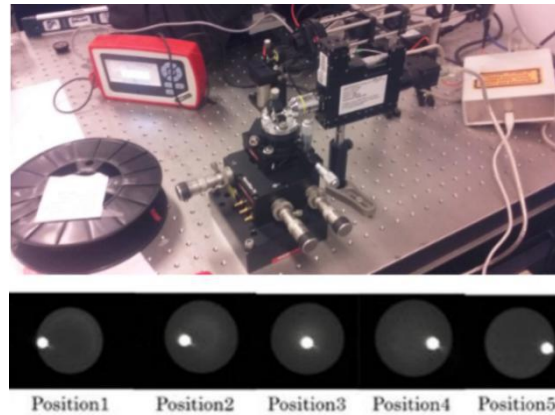


Figure 13: Input beam position captured by PSM

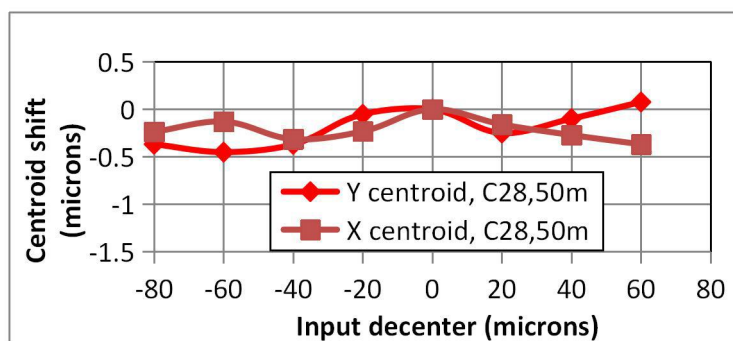


Figure 14: The measured centroid of CeramOptec high NA 2m fiber

It is shown that the maximum Peak to valley (PV) of the centroid in both x and y direction is less than $1\mu\text{m}$ and its standard deviation is less than $0.3\mu\text{m}$: even though the range of the movement is the full width of the fiber. Note that for a longer length of same fiber, the scrambling performance will be even better.

We also examined the effect of the incidence beam angle on the near field distribution. Figure 15 shows the centroid shift when incidence varies from -7° to $+8^\circ$. The tested fiber is high NA 50m CeramOptec fiber and angle step is 1° . The measured maximum PV is about $1.26\mu\text{m}$ and its standard deviation is even less than $0.5\mu\text{m}$: note that the angular range is much bigger than real telescope operation. For more plausible variations of $\pm 2^\circ$, the variations are again less than $1\mu\text{m}$. To summarize, for typical fiber lengths, the near field centroid is affected by plausible lateral and angular position of the incidence beam, by less than 1% of the fiber diameter.

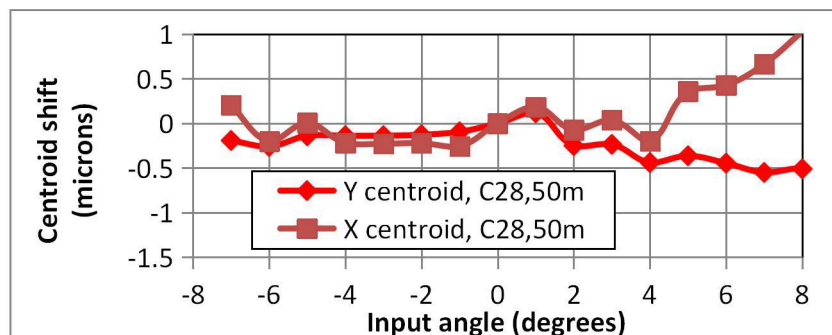


Figure 15: The measured centroid of CeramOptec high NA 50m fiber vs incidence angle, together with a sample of the actual near-field images.

The results shown in Figure 15 are for an underfilled beam input. We repeated the test for an overfilled NA=0.25 input at varying angles. This was specifically to address concerns that the output near-field may

depend on the non-telecentricity of the input beam [9]. For input beam tilts of a few degrees, we found motions in the centroids to be $\pm 1\mu\text{m}$ level, as shown in Figure 16(a), and consistent with measurement error.

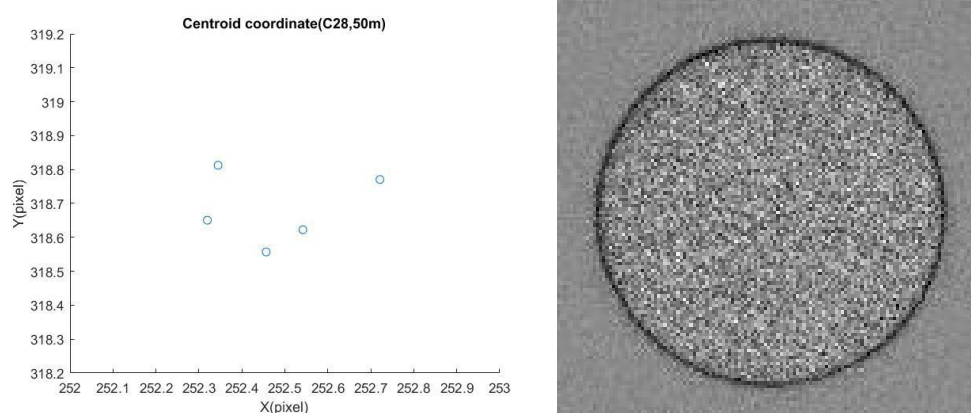


Figure 16 (a). X and Y centroid positions for $0^\circ, \pm 1^\circ, \pm 2^\circ$ input tilts. Pixel size is $5.5\mu\text{m}$. Figure 16 (b). Difference between renormalized output near-field images on $-axis$ vs tilted at 2° . Grey scaling is $\pm 5\%$. Input beam was overfilled $NA=0.25$. Fiber was 50m CeramOptec high-NA.

We also looked in more detail at changes in the near-field image. Figure 16(b) shows the difference between the near-field images with on-axis input, vs 2° off-axis. Any differences are $<0.5\%$, being invisible at the level of residual speckle noise.

7. CONCLUSIONS AND FURTHER WORKS

In this paper, we have presented measurements of the FRD, throughput and scrambling performance of high NA fiber from Polymicro and CeramOptec, when used at NA of 0.25. The FRD performance of the CeramOptec fiber is acceptable for astronomical use, though the Polymicro fiber was much less good. The attenuation performance of both sets of fibers was close to the manufacturer's estimates, and actually better in the NIR. Plausible variations of the input near- and far-field beam leads to variations in the output near-field centroid of less than 1% of the fiber diameter.

From our measurements to date, it looks as if the CeramOptec high NA fiber is suitable, in terms of FRD, throughput and scrambling, for use at $f/2$, as needed for direct use at the prime focus of the MSE telescope. Some further tests would be beneficial: we have not understood the drop in throughput as a function of collimated input angle; and also we have only demonstrated good throughput over the range 395nm-1550nm. There is a possibility that the attenuation beyond $\sim 1600\text{nm}$ could increase because of evanescent losses from the finite cladding thickness ($20\mu\text{m}$) and operation close to the NA of the fiber (where the required cladding thickness becomes infinite). Also, the fibers used for MSE may be smaller and with thinner cladding. However, the Polymicro high NA fiber, with just $10\mu\text{m}$ cladding, shows only marginally increased attenuation between 1310nm and 1550nm, and an increase is expected in any case due to OH content. Hence, it seems that evanescent losses are not severe even at cladding thickness/wavelength ratios well below the nominal guideline value of 10. This would mean that CeramOptec high NA fiber, with core/clad ratio 1:1.4, would be suitable to $1.8\mu\text{m}$, for any plausible fiber core diameter (say $75\mu\text{m}$ - $125\mu\text{m}$).

ACKNOWLEDGEMENTS

Many thanks to Graham Murray for advice on fiber termination. Thanks also to China Scholarship Council, which paid for KaiYuan Zhang to come to AAO, and thanks to Jon Lawrence at AAO for supporting this project.

REFERENCES

- [1] J. Pazder, P.Fournier,R. Pawluczyk and M.V.Kooten, “The FRD and transmission of the 270-m GRACES optical fiber link and a high numerical aperture fiber for astronomy”, *Proc.SPIE* 9151, 915124-10 (2014)
- [2] D. M. Haynes,M. J.Withford, J. M. Dawes, J. S. Lawrence and R. Haynes, “Relative contributions of scattering, diffraction and modal diffusion to focal ratio degradation in optical fibres”, *Mon. Not. R. Astron. Soc.* 414, 253–263 (2011)
- [3] J. Allington-Smith, G.Murray and U. Lemke, “Simulation of complex phenomena in optical fibres”, *Mon. Not. R. Astron. Soc.* 427, 919–933 (2012)
- [4] A. D. Eigenbrot, M.A. Bershady and C. M. Wood, “Impact of surface-polish on the angular and wavelength dependence of fiber focal ratio degradation”, *Proc.SPIE*, 8446, 84465-84475 (2012)
- [5] L.Crausea, M. Bershadyb and D.Buckleya, “Investigation of focal ratio degradation in optical fibres for astronomical instrumentation”, *Proc.SPIE*, 7014, 70146C1-70146C11 (2008)
- [6] J. D. Murphy, P.J. MacQueen, G. J. Hill, F. Grupp, A. Kelz, P. Palunase, M. Roth and A. Fry, “Focal Ratio Degradation and Transmission in VIRUS-P Optical Fibers”, *Proc.SPIE*, 7018, 788411-788423 (2008)
- [7] J. Allington-Smith, C. Dunlop, U. Lemke, G. Murray, “End effects in optical fibres”, *MNRAS*, 436, 3492 (2013)
- [8] Polymicro Technologies,“The Book on the technologies of Polymicro”, online at www.polymicro.com/mx_upload/superfamily/polymicro/theBOOK.pdf
- [9] Poppett,C.L., Edelstein,J., Besuner, R., Silber,J.H.,“Focal ration degradation performance of fiber position technology used in the Dark Energu Spectroscopic Instrument(DESI)”, *Proc.SPIE*, 9147, 914763 (2014)